NeuroImage: Clinical 34 (2022) 103026

Contents lists available at ScienceDirect

NeuroImage: Clinical

journal homepage: www.elsevier.com/locate/ynicl

Specific structuro-metabolic pattern of thalamic subnuclei in fatal familial insomnia: A PET/MRI imaging study

Kexin Xie [a], Yaojing Chen [b], Min Chu [a], Yue Cui [a], Zhongyun Chen [a], Jing Zhang [a], Li Liu [a,c], Donglai Jing [a,d], Chunlei Cui [e], Zhigang Liang [e], Liankun Ren [a], Pedro Rosa-Neto [f], Imad Ghorayeb [g,h,i], Zhanjun Zhang [b,1,*], Liyong Wu [a,j,1,*]

[a] Department of Neurology, Xuanwu Hospital, Capital Medical University, Beijing 100053, China
[b] State Key Laboratory of Cognitive Neuroscience and Learning, Beijing Normal University, Beijing 100875, China
[c] Department of Neurology, Shenyang Fifth People Hospital, Shenyang, Liaoning 110023, China
[d] Department of Neurology, Rongcheng People's Hospital, Baoding, Hebei 071700, China
[e] Department of Nuclear Medicine, Xuanwu Hospital, Capital Medical University, Beijing 100053, China
[f] McGill University Research Centre for Studies in Aging, Montreal, QC H3G 1Y6, Canada
[g] Université de Bordeaux, Institut de Neurosciences Cognitives et Intégratives d'Aquitaine, UMR 5287, F-33076 Bordeaux, France
[h] CNRS, Institut de Neurosciences Cognitives et Intégratives d'Aquitaine, UMR 5287, F-33076 Bordeaux, France
[i] Département de Neurophysiologie Clinique, Pôle Neurosciences Cliniques, CHU de Bordeaux, F-33076 Bordeaux, France
[j] National Clinical Research Center for Geriatric Diseases, Beijing 100053, China

ARTICLE INFO

Keywords:
Fatal familial insomnia
Magnetic resonance imaging
18F-Fluorodeoxyglucose
Positron-Emission Tomography
Thalamic nuclei

ABSTRACT

Background: Dysfunction of the thalamus has been proposed as a core mechanism of fatal familial insomnia. However, detailed metabolic and structural alterations in thalamic subnuclei are not well documented. We aimed to address the multimodal structuro-metabolic pattern at the level of the thalamic nuclei in fatal familial insomnia patients, and investigated the clinical presentation of primary thalamic alterations.

Materials and Methods: Five fatal familial insomnia patients and 10 healthy controls were enrolled in this study. All participants underwent neuropsychological assessments, polysomnography, electroencephalogram, and cerebrospinal fluid tests. MRI and fluorodeoxyglucose PET were acquired on a hybrid PET/MRI system. Structural and metabolic changes were compared using voxel-based morphometry analyses and standardized uptake value ratio analyses, focusing on thalamic subnuclei region of interest analyses. Correlation analysis was conducted between gray matter volume and metabolic decrease ratios, and clinical features.

Results: The whole-brain analysis showed that gray matter volume decline was confined to the bilateral thalamus and right middle temporal pole in fatal familial insomnia patients, whereas hypometabolism was observed in the bilateral thalamus, basal ganglia, and widespread cortices, mainly in the forebrain. In the regions of interest analysis, gray matter volume and metabolism decreases were prominent in bilateral medial dorsal nuclei, anterior nuclei, and the pulvinar, which is consistent with neuropathological and clinical findings. A positive correlation was found between gray matter volume and metabolic decrease ratios.

Conclusions: Our study revealed specific structuro-metabolic pattern of fatal familial insomnia that demonstrated the essential roles of medial dorsal nuclei, anterior nuclei, and pulvinar, which may be a potential biomarker in diagnosis. Also, primary thalamic subnuclei alterations may be correlated with insomnia, neuropsychiatric, and autonomic symptoms sparing primary cortical involvement.

Abbreviations: FFI, Fatal familial insomnia; PRNP, prion protein; FDG, fluorodeoxyglucose; MMSE, Mini-Mental State Examination; MoCA, Montreal Cognitive Assessment; CDR, Clinical Dementia Rating; PSG, polysomnography; MR, magnetic resonance; GM, Gray matter; CAT, Computational Anatomy Toolbox; SPM12, Statistical Parametric Mapping 12; VBM, voxel-based morphometry; SUVR, Standardized uptake value ratios; GMV, GM volume; ROI, region of interest; DARTEL, Diffeomorphic Anatomical Registration Through Exponentiated Lie Algebra; MNI, Montreal Neurological Institute.

* Corresponding authors at: Department of Neurology, Xuanwu Hospital, Capital Medical University, Beijing 100053, China.
E-mail addresses: zhang_rzs@bnu.edu.cn (Z. Zhang), wmywly@hotmail.com (L. Wu).

[1] These authors contributed equally to this work.

https://doi.org/10.1016/j.nicl.2022.103026
Received 4 January 2022; Received in revised form 31 March 2022; Accepted 24 April 2022
Available online 26 April 2022

1. Introduction

Fatal familial insomnia (FFI) is a rare but invariably fatal disease that is caused by the D178N-129M mutation of the prion protein (*PRNP*) gene, which is clinically characterized by progressive insomnia, dysautonomia, motor dysfunction, and cognitive deterioration (Khan and Bollu, 2020; Llorens, Zarranz, Fischer, Zerr, & Ferrer, 2017; Megelin, Thomas, Ferrer, & Ghorayeb, 2017; W et al., 2018). Considerable effort has been made to understand the pathophysiological mechanisms of FFI over the past decades. Postmortem analyses have revealed the selective involvement of the thalamus in patients with FFI, which manifests as neuronal loss and astrogliosis. Remarkably, alterations of the thalamus have been previously reported in predominantly the medial dorsal nuclei, anterior ventral nuclei, and pulvinar (Gambetti, Parchi, Petersen, Chen, & Lugaresi, 1995; Jansen et al., 2011; Llorens et al., 2017; Peng, Zhang, Dong, & Lu, 2015). Currently, the dysfunction of the thalamus is considered the core of FFI.

Neuroimaging has been used to study patients with FFI to investigate brain alterations. Previous studies have used MRI and fluorodeoxyglucose (FDG)-PET to quantify brain degeneration in patients with FFI. Although MRI is considered a less sensitive examination for detecting nonspecific atrophy,(Chen et al., 2018; Khan and Bollu, 2020) studies have reported volume decline that is confined to the thalamus (Grau-Rivera et al., 2017; Krasnianski et al., 2008; Llorens et al., 2017). Notably, metabolic changes are considered a prominent diagnostic characteristic (W et al., 2018); hypometabolism has been observed in the thalamus in symptomatic and presymptomatic patients (Cortelli et al., 2006; Cortelli et al., 1997; Manetto et al., 1992; Shi et al., 2010). Although the selective thalamic alterations detected using neuroimaging analyses are considered a conspicuous clinical feature of FFI, imaging research at the level of the thalamic nuclei remains scarce. The inconsistencies between neuroimaging and neuropathological findings suggest that further neuroimaging assessments will be extremely valuable.

Given the current paucity of neuroimaging studies on specific thalamic subnuclei and insufficient appliance in diagnosis, we conducted a multimodal neuroimaging analysis in patients with FFI to investigate structural and metabolic spatial pattern in the thalamic subnuclei. Also, taking FFI as an ideal model of primary thalamic involvement, we investigated the clinical manifestations of primary thalamic alterations.

2. Materials and methods

2.1. Participants

Five patients with FFI were identified and enrolled from the Department of Neurology of Xuanwu Hospital from 2017 to 2019. All patients underwent detailed clinical interviews, physical examinations, and neuropsychological assessments within 1 month of recruitment. Standard clinical and cognitive assessments included the Mini-Mental State Examination (MMSE), Montreal Cognitive Assessment (MoCA), and the Clinical Dementia Rating (CDR). Family history was obtained from all patients with FFI, and *PRNP* genotype was determined through direct sequencing. In addition, polysomnography (PSG), electroencephalogram (EEG), and cerebrospinal fluid (CSF) were tested. Final diagnoses of patients with FFI were determined according to expert consensus on the clinical diagnostic criteria for FFI (W et al., 2018). Exclusion criteria included: 1) presence of other causes of cognitive impairment, including small vessel disease, stroke, infection, autoimmune diseases, metabolic diseases, and other neurodegenerative diseases except for FFI; 2) inability to cooperate; 3) history of traumatic brain injury; 4) history of psychosis or congenital mental growth retardation; and 5) contradiction to MRI and PET. Ten age- and sex-matched healthy controls were enrolled from the community. Exclusion criteria were as follows: 1) primary complaint of memory decline or objective memory impairment with cutoff scores of 19 (no formal education), 22 (1 to 6 years of education), and 26 (seven or more years of education) for the MMSE; cutoff scores of 13 (no formal education), 19 (1 to 6 years of education), and 24 (seven or more years of education) for the MoCA; and a CDR score of ≥ 0.5; 2) presence of psychiatric disorders (neuropsychiatric inventory ≥ 1); 3) history of other neurologic disorders; 4) history of traumatic brain injury; 5) history of psychosis or congenital mental growth retardation; 6) contraindications to MRI and PET; 7) any form of mutation in the *PRNP* gene; or 8) any occurrence of prion disease within the family pedigree. All healthy controls were clinically screened to exclude individuals uncooperative for neuroimaging analysis.

2.2. Standard protocol approvals, registrations, and patient consents

The clinical protocols and informed consent were approved by the ethics committee and local institutional review board of Xuanwu Hospital, Capital Medical University, China. The study was performed under the relevant guidelines and regulations. All participants enrolled in the study or their guardians provided informed written consent prior to the commencement of the study. Authorization was obtained for disclosure of any recognizable persons in any information that may be published in the journal.

2.3. Multimodal imaging scanning and image parameters

Magnetic resonance (MR) scanning was performed on a GE Signa PET/MR 3.0 Tesla scanner (GE Healthcare, Milwaukee, WI) at Xuanwu Hospital, Capital Medical University. A three-dimensional T1-weighted fast field echo sequence (repetition time = 25 ms, echo time = 4.6 ms, flip angle = 30°, 220 contiguous axial slices with a voxel size = 0.89 × 0.89 × 0.8 mm, matrix size = 256 × 256, and a field of view = 230 × 182 mm) was used for data acquisition. One patient was not cooperative during the scanning. Therefore, only four patients with FFI were scanned from 2017 to 2019.

PET scans were acquired at Xuanwu Hospital using a GE Signa PET/MR 3.0 Tesla scanner (GE Healthcare, Milwaukee, WI). All five patients with FFI and 10 healthy controls underwent PET scans from 2017 to 2019. The ^{18}F-FDG PET images were acquired over 15 min, following a bolus intravenous injection of ^{18}F-FDG (approximately 308 MBq) with an uptake time of 30 min. Images were reconstructed using an ordered subset expectation maximization algorithm with 16 subsets and four iterations.

2.4. Data processing and analysis

2.4.1. Structural MRI preprocessing and analysis

All T1-weighted images were pre-processed using the Computational Anatomy Toolbox (CAT12, https://dbm.neuro.uni-jena.de/cat12/) toolbox segment data pipeline, which is implemented within Statistical Parametric Mapping 12 (SPM12; https://www.fil.ion.ucl.ac.uk/spm) in Matlab (R2015a; MathWorks, Inc., Natick, MA). The images were bias-corrected, tissue classified, and normalized to the Montreal Neurological Institute (MNI) 3 mm isotropic voxel resolution, based on tran xel resolution using linear (12-parameter affine) and nonlinear transformations within a unified model and applying high-dimensional Diffeomorphic Anatomical Registration Through Exponentiated Lie Algebra (DARTEL) normalization (Ashburner, 2007; Mechelli et al., 2005). Gray matter (GM), white matter, and CSF segments were modulated to preserve local tissue amounts. After quality assurance and homogeneity inspections, all images were smoothed with a Gaussian kernel of 8 mm full-width-half-maximum. To compare patterns of GM atrophy between patients with FFI and controls, voxel-based morphometry (VBM) analyses were conducted using a two-sample *t*-test, with age, sex, and years of education as covariates. Significance was set at $p < 0.00001$.

2.4.2. ^{18}F-FDG PET preprocessing and analysis

PET image processing and analyses were performed using SPM12 implemented in Matlab software. The scans of each participant were spatially normalized into Montreal Neurological Institute (McGill University, Montreal, QC, Canada) standard space, interpolated to 2 mm isotropic voxel size, and smoothed with an 8-mm Gaussian kernel. Standardized uptake value ratios (SUVR) were calculated using cerebellar GM as a reference region for preprocessed ^{18}F-FDG PET images. Then, a voxel-wise comparison of the SUVR was conducted between the patients with FFI and healthy controls, with age and sex as covariates. A two-sample *t*-test was used and the significance level was set at $p < 0.00001$ (two-sided).

2.4.3. Regions of interest analysis at the thalamic nuclei level

To further explore the effect of FFI on GM volume (GMV) and metabolism of the thalamic nuclei, we used the Talairach Atlas (https://www.talairach.org) to classify the thalamic nuclei and performed a region of interest (ROI) analysis. Specifically, we defined 20 ROIs (10 in each hemisphere): ventral posterior medial nucleus, ventral posterior lateral nucleus, medial dorsal nucleus, pulvinar, ventral lateral nucleus, ventral anterior nucleus, anterior nucleus, lateral posterior nucleus, lateral dorsal nucleus, and midline nucleus. Then, covariance analysis was used to compare the metabolism and GMV of the thalamic nuclei between patients with FFI and controls after adjusting for age, sex, and education.

2.5. Statistics

The SPSS software (version 23.0, IBM Inc., New York, NY) and GraphPad Prism software (version 8.3.0, GraphPad Software Inc, La Jolla, CA) were used to evaluate statistical significance. Differences in age and education were assessed using Student's *t*-test. Sex differences were assessed using a chi-square test. Differences in cognitive scores were assessed using Student's *t*-test. Pearson's correlation analysis was performed for the thalamus subnuclei between the decrease ratio of metabolism and GMV. We defined the decrease rate as the ratio of the GMV or SUVR difference between healthy controls and patients with FFI to that of healthy controls. Results were considered statistically significant at $p < 0.05$. Spearman's correlation analysis was performed between clinical features and the decrease ratio of metabolism and GMV in thalamic subnuclei, and the clinical features include disease prognosis, disease onset, disease duration, total sleep time, and periodic limb movement index (PLMI). Given the limited sample size, results were considered statistically significant at $p < 0.1$.

2.6. Ethics statement

The study protocols outlined in this manuscript were approved by the Ethics Committee and local Institutional Review Board of Xuanwu Hospital, Capital Medical University, Beijing. All methods and experiments were performed following the relevant guidelines and regulations. All participants enrolled in the study or their guardians signed an informed written consent giving specific approval for this study before the study commenced.

3. Results

3.1. Participants populations and clinical features

All five patients with FFI (two males and three females) had a positive family history and a *PRNP* D178N-129 M mutation. Detailed demographic and neurological assessment scores are summarized in Table 1. There were no significant differences in age, sex, or years of education between the patients with FFI and healthy controls. According to the 2018 Expert Consensus, (W et al., 2018) all five patients with FFI showed cluster A-sleep-related symptoms. Cluster B-neuropsychiatric- and cluster C-progressive-sympathetic symptoms were present in most patients, whereas rapidly progressive dementia, sweating, and tachycardia existed in all five patients. CSF 14–3-3 analysis was negative in all patients. Periodic synchronous discharges on EEG or cortical/basal ganglia hyperintensity on DWI and FLAIR imaging were not detected in any patients. PSG showed that all patients had significantly reduced duration of rapid eye movement sleep and laryngeal stridor. The mean survival time was 14 months for the five patients with FFI. Only 4 patients completed PSG examination, as case 2 conducted portable sleep monitoring device. The clinical features and polysomnography results are summarized in Table 2.

Table 1
Demographic data of patients with FFI and healthy controls.

	FFI patients	Healthy controls	T (χ^2)	*p* value
Number of subjects	5	10	–	–
Age	55 ± 11.1	57 ± 5.2	−0.46	0.65
Gender (Male/Female)	2/3	5/5	0.734*	0.71*
Years of education	12 ± 5.1	11 ± 2.8	0.10	0.94

Data are presented as means ± standard deviations.
*The *p* value for gender was obtained using a χ^2 test.

3.2. Whole brain VBM analyses

As shown in Fig. 1A, in patients with FFI, the VBM analysis ($p < 0.00001$) revealed limited regions of atrophy compared with healthy controls, which were confined to the bilateral thalamus and right middle temporal pole. No regions of volume increase were observed in patients with FFI. Detailed data are summarized in Supplementary Table 1.

Table 2
Demographic and clinical data of five patients with FFI.

	Case 1	Case 2	Case 3	Case 4	Case 5
Gender	M	F	F	M	F
Age at onset (years)	55	39	64	49	66
Onset to diagnosis (months)	11	9	7	6	9
Disease duration (months)	15	18	13	10	14
Clinical Features					
Cluster A–sleep-related symptoms					
Insomnia	+	+	+	+	+
Sleep-related involuntary movements#	+	+	+	+	+
Sleep-related dyspnea	+	+	+	+	+
Laryngeal stridor	+	+	+	+	+
Cluster B–neuropsychiatric symptoms					
Rapidly progressive dementia	+	+	+	+	+
Psychiatric symptoms#	+	–	+	+	+
Ataxia	+	+	–	+	+
Parkinsonism	+	–	–	–	–
Cluster C–progressive autonomic symptoms					
Hypertension	–	+	–	+	+
Hyperhidrosis	+	+	+	+	+
Tachycardia	+	+	+	+	+
Irregular breathing	–	+	–	–	+
PSG					
Total sleep time (min)	11.0	NA	290.0	310.0	309.0
REM (%)	0.0	NA	9.7	17.4	6.5
REM latency (min)	–	NA	99.0	217.0	189.0
PLMI	272.7	NA	117.3	213.5	172.8

Normal range of PSG: Total sleep time: > 360 min; REM (%): 20–25; REM latency (min): 70–90; PLMI: ≤ 25.
+: symptom/sign observed, −: symptom/sign not observed.
: Sleep-related involuntary movements included frequent changes in body position and twitchy non-purposeful movements of limbs during sleep. Psychiatric syndromes included hallucination, personality change, depression, anxiety, aggressiveness, and disinhibition.

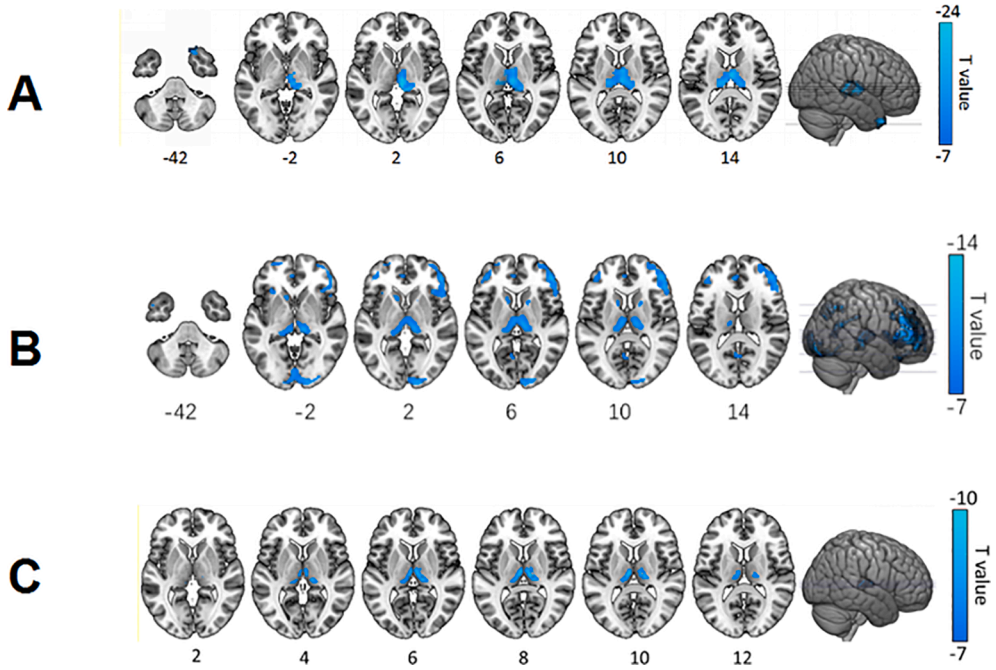

Fig. 1. Whole-brain VBM and FDG-PET analyses comparing patients with FFI and healthy controls showed bilateral thalamus and cortical alterations. Significant areas of volume loss in patients with FFI compared with healthy controls ($p < 0.00001$). (**B**) Areas of significant hypometabolism in patients with FFI compared with healthy controls ($p < 0.00001$). (C) Significant areas of volume loss in FFI patients applying thalamus mask ($p < 0.00001$).

From the whole brain GMV analysis, we found that the thalamus is the key brain region of FFI in neuroimaging alterations by selective thalamic involvement, so we further explored the effect of FFI on thalamic metabolism.

3.3. FDG-PET analyses

In patients with FFI, voxel-wise examinations ($p < 0.00001$) revealed hypometabolism in the bilateral thalamus, bilateral cingulum, the frontal, parietal, and temporal lobes, left insula, and bilateral caudate compared with healthy controls. Regions with significant metabolic changes are shown in Fig. 1B. Detailed data are provided in Supplementary Table 2.

To more focus on the thalamus, we applied a thalamic mask in VBM analysis, and found hypometabolism in the left medial dorsal nuclei and right pulvinar ($p < 0.00001$). Regions of significant changes are shown in Fig. 1C. Detailed data are shown in Supplementary Table 3.

3.4. ROI analyses of the thalamic nuclei

Having discovered the selective thalamic involvement by whole brain analysis, we conducted ROI analyses to further investigate the subnuclei alterations.

The thalamic atlas is shown in Fig. 2A. After applying the ROI masks, significant GMV loss was observed in most thalamic nuclei for the uncorrected analysis ($p < 0.001$) and was most pronounced in the right medial dorsal nuclei, right anterior nucleus, and right pulvinar. Detailed GMV changes at the level of thalamic nuclei are summarized in Fig. 2B and Fig. 3A and Supplementary Table 4.

In patients with FFI, the FDG-PET analysis ($p < 0.001$) showed hypometabolism in multiple clusters, which was prominent in the bilateral medial dorsal nucleus, left pulvinar, and right lateral posterior nucleus, as shown in Fig. 2C and 3B and Supplementary Table 5.

Overlapping areas of GMV and metabolic changes are shown in Fig. 2D, which were most pronounced in the bilateral medial dorsal nuclei, anterior nuclei, and pulvinar.

3.5. Correlation analysis

In patients with FFI, the correlation analysis showed a positive correlation between the metabolism decrease rate and GMV decrease rate ($r = 0.5009$, $p = 0.0005$). Scatter plots are shown in Fig. 4. Also, the correlation analysis ($r = -0.8000$, $p = 0.1333$) showed a trend between disease duration and the metabolism decrease ratios of medial dorsal nuclei, anterior nuclei as well as pulvinar. Scatter plots are shown in Supplementary Fig. 1. Additionally, correlation analyses were conducted between GMV decrease ratios and metabolism decrease ratios in each ROI, unfortunately, no supportive results were shown.

4. Discussion

By applying whole-brain and ROI analyses, we revealed distinct structural and metabolic thalamic alterations, profound in the medial dorsal nuclei, anterior nuclei, and pulvinar, which is consistent with neuropathology findings. Furthermore, our results suggested a specific structuro-metabolic pattern of thalamic subnuclei, which may be a potential biomarker in clinical diagnosis.

Numerous previous studies have suggested non-specific cortical atrophy without distinctive thalamic alterations (He et al., 2019; Rupprecht et al., 2013; Sun et al., 2017). While our study revealed distinctive structuro-metabolic pattern in FFI subnuclei. Furthermore, our study showed pathological findings in vivo by non-invasive methods. The GMV alterations met the pathological findings of previous research, (Khan and Bollu, 2020; Montagna, 2011) while the metabolic pattern fit the thalamolimbic circuits. Moreover, applying the hybrid PET/MRI system allowed us to match the structural and metabolic alterations in the same individual, which provided a comprehensive illustration of brain changes in patients with FFI.

The thalamus changes detected in our study were also found in previous research. Previous FDG-PET studies reported hypometabolism in the bilateral thalamus, cingulum, cortices, and basal ganglia,(Khan and Bollu, 2020; Provini, 2013; Zhang et al., 2010) which is in line with our results (Cortelli et al., 1997; Provini, 2013; Rupprecht et al., 2013; Tham, Thian, Ratnagopal, & Xie, 2018). As for thalamic subnuclei,

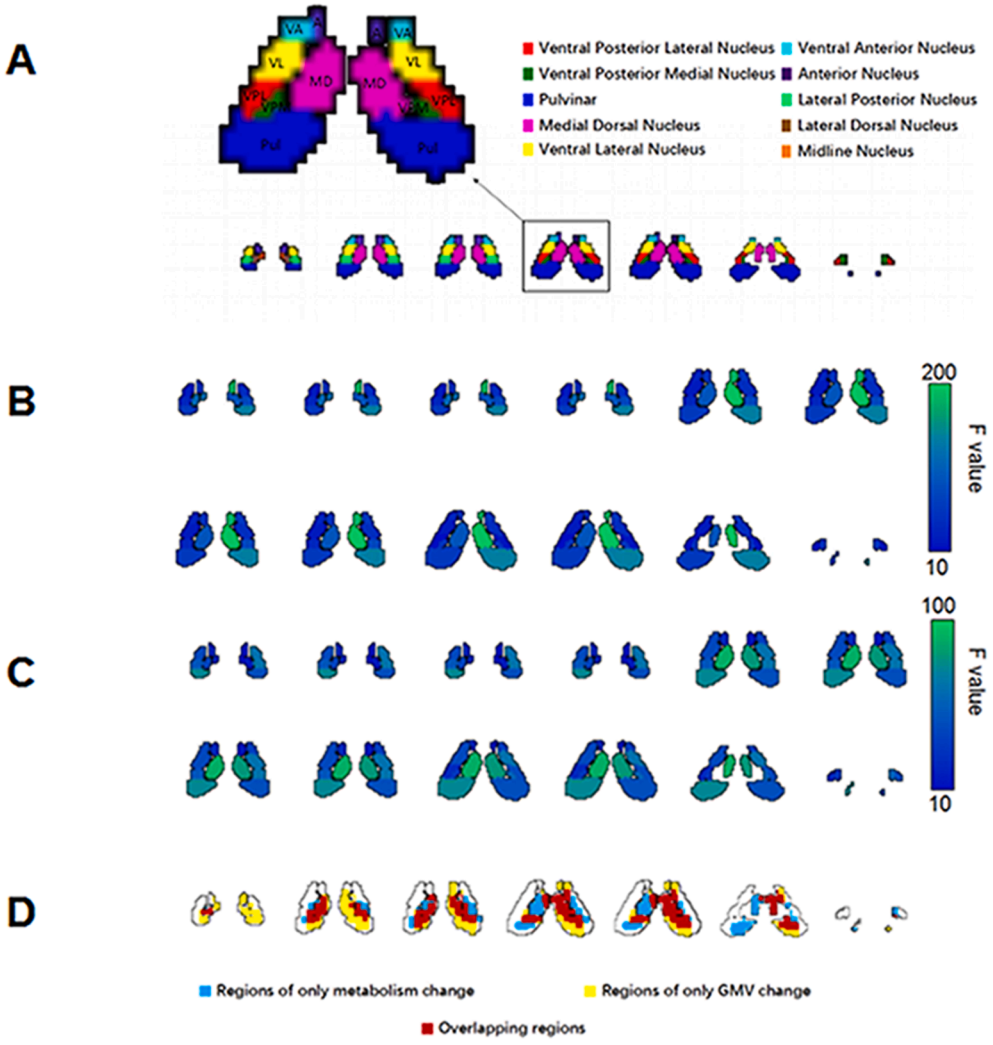

Fig. 2. ROI analysis of the thalamic nuclei comparing patients with FFI and healthy controls showed multiple nuclei involvement predominantly in medial dorsal nuclei, anterior nuclei and pulvinar. (**A**) ROIs according to the Talairach Daemon atlas. (**B**) Significant areas of GMV loss in patients with FFI compared with healthy controls ($p < 0.00001$). (**C**) Areas of significant hypometabolism in patients with FFI compared with healthy controls ($p < 0.00001$). (**D**) Overlapping regions of both GMV and metabolic changes in patients with FFI.

current neuroimaging analysis remains scarce, whereas postmortem analyses have indicated medial dorsal and anterior ventral nuclei involvement, followed by involvement of the pulvinar and inferior olives,(Haïk et al., 2008; Khan and Bollu, 2020; Llorens et al., 2017) which supports our ROI analysis results. In addition, a positive correlation between GMV decrease and metabolism decrease ratios in the thalamic subnuclei was observed, which suggested corresponding atrophy and hypometabolism patterns. Previous neuropathological research has reported focal neuronal loss, spongiosis, astrogliosis, and prion protein deposition in the thalamus, which are most prominent in the medial dorsal and anterior ventral nuclei (Khan and Bollu, 2020; Montagna, 2011). Such alterations induce volume decrease and hypometabolism as functions and connections diminish. More diffusive hypometabolism areas were also investigated in FFI patients than structural brain damage. Functional alterations have always been considered prior to structural alterations. In our research, more diffusive hypometabolism, especially in cortical areas, were observed. Previous researches have found nonspecific cortical atrophy and neuronal loss in post-mortem analysis, which related to a relatively late stage of disease (Khan and Bollu, 2020; Montagna, 2011). The diffusive hypometabolism may be related to the disease course, while the simultaneous structural and metabolic changes in thalamus may suggest which is the core area in FFI.

Our study found profound thalamic alterations in predominantly the medial dorsal nuclei, anterior nuclei, and pulvinar using ROI analysis, alongside changes in the cingulum and forebrain cortices using whole-brain analysis. The involvement of these regions corresponds with the pattern of thalamo-limbic circuitry. Moreover, all our patients with FFI presented with clinical changes, which included sleep-related, neuropsychiatric, and automatic symptoms, which are consistent with thalamus lesions. The thalamus is considered an essential fulcrum in the pathology of FFI. Studies have shown that the thalamus has connections with the forebrain limbic areas, subcortical hypothalamus, and brainstem regions and functions as a relay station in thalamo-limbic circuits (Jan, Reiter, Wasdell, & Bax, 2009). Among all the thalamic nuclei, the medial dorsal nucleus is one of the higher order for its close anatomical relationship with the entire prefrontal cortex and as it also receives broad spectrum of afferent projections from the areas involved in regulation of sleep wake cycle (Van der Werf et al., 2002). Lesions within this nucleus may release the subcortical and brainstem regions from forebrain cortical control, which leads to autonomic, motor activation and “prefrontal-like” dysexecutive symptoms (Montagna, 2011; Van der Werf et al., 2000). The hyperactivity of the reticular regions of the brainstem could also result in insomnia, and loss of sleep spindles (Jan et al., 2009; Montagna, 2011). Additionally, correlations between the medial dorsal nuclei and memory have been reported (Marini, Imeri, & Mancia, 1988; Markowitsch, 1981; Watanabe & Funahashi, 2012) as well as between the anterior nuclei and working memory (Hamani et al., 2010; Oh et al., 2012), and between the pulvinar and visual attention (Smith, Cotton, Bruno, & Moutsiana, 2009). In our patients, all sleep-related symptoms (5/5), hyperhidrosis (5/5), and tachycardia (5/5) could be consistent with medial dorsal nuclei dysfunction-related symptoms, whereas rapidly progressive dementia (5/5) and

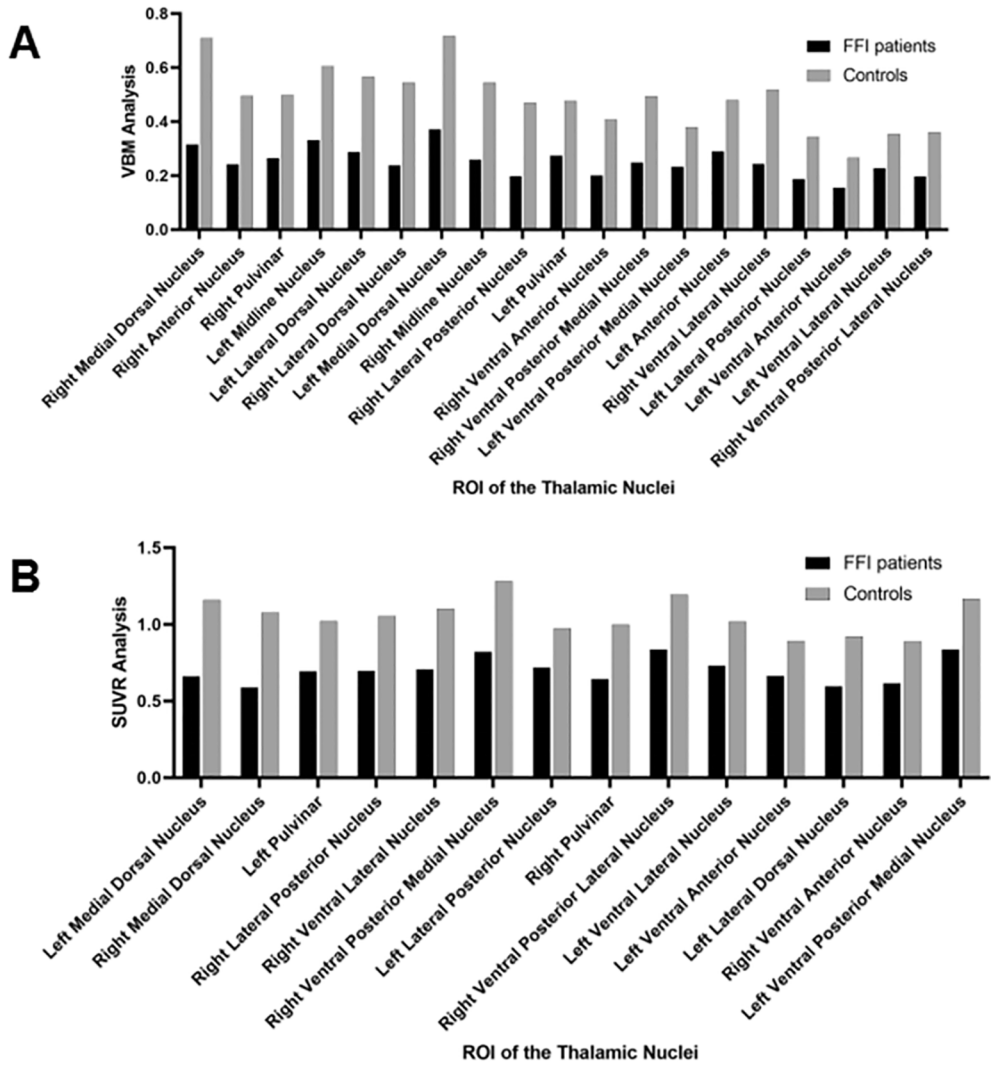

Fig. 3. GMV and metabolism changes in thalamic nuclei ROIs. (**A**) Significant areas of GMV change in the thalamic nuclei in patients with FFI compared with healthy controls ($p < 0.001$). (**B**) Significant areas of metabolism change in the thalamic nuclei in patients with FFI compared with healthy controls ($p < 0.001$).

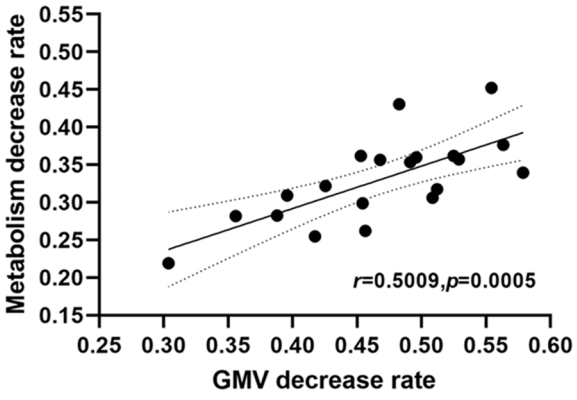

Fig. 4. A positive correlation was found between GMV decrease rate and metabolic decrease rate ($r = 0.5009$, $p = 0.0005$).

psychiatric symptoms (4/5) could be explained by anterior nuclei, pulvinar and also medio dorsal nuclei involvement. It could be hypothesized that these nuclei alteration plays a significant role in disease onset and progression. Also, the metabolic pattern showed both thalamic and forebrain cortical involvement, which corresponds to the thalamolimbic circuit. With structural alterations consistent with pathological findings, a specific structuro-metabolic pattern was pictured in FFI.

Aside from the selective thalamus alterations, atrophy in right middle temporal pole has also been observed in FFI patients. Nonspecific cortical atrophy has been reported in previous researches which may be related to the disease process (Chen et al., 2018; Khan and Bollu, 2020). Also, one of our 5 FFI patients showed asymmetrical atrophy in the right hemisphere, which may lead to this nonspecific alteration in right middle temporal.

Due to the low prevalence of FFI, only a small number of patients were enrolled in our research. Thus, no significant different was detected in spearman's analysis, and the results didn't correct for multiple comparison. But, one would expect to find a significant correlation between more clinical features and subnuclei alterations, and between volume and metabolism decrease ratio in each ROI with an enlarged sample size. Also, as our analysis has revealed a positive correlation between the decrease ratios of GMV and metabolism, we expected to conduct partial volume correction to further discuss the relationship between metabolism and GMV, while some published studies also skipped the correction(Jack et al., 2017; Knopman et al.,). Furthermore, we did not perform postmortem analyses on our patients with FFI. For future studies in patients with FFI, we aim to collect additional data in more patients to further understand the disease.

5. Conclusion

Our study demonstrated spatial-specific structural and metabolic thalamic nuclei changes, especially in the medial dorsal nuclei, anterior nuclei, and pulvinar using multimodal neuroimaging examinations. Detecting characteristic thalamic subnuclei alterations and the specific structuro-metabolic pattern in patients with FFI using multimodal neuroimaging techniques has the potential to improve the diagnosis of FFI. Also, the primary thalamic alterations in medial dorsal nuclei, anterior nuclei and pulvinar may result in insomnia, neuropsychiatric and autonomic symptoms, sparing primary cortical involvement.

6. Data and code availability

The data that support the findings of this study are available from the corresponding author upon reasonable request.

CRediT authorship contribution statement

Kexin Xie: Conceptualization, Formal analysis, Investigation, Writing – original draft. **Yaojing Chen:** Formal analysis, Methodology. **Min Chu:** Formal analysis, Methodology, Writing – review & editing. **Yue Cui:** Conceptualization, Writing – review & editing. **Zhongyun Chen:** Writing – review & editing. **Jing Zhang:** Funding acquisition. **Li Liu:** Conceptualization, Funding acquisition. **Donglai Jing:** Methodology. **Chunlei Cui:** Methodology. **Zhigang Liang:** Funding acquisition. **LianKun Ren:** Conceptualization, Methodology, Writing – review & editing. **Pedro Rosa-Neto:** Methodology, Writing – review & editing. **Imad Ghorayeb:** Methodology, Writing – review & editing. **Zhanjun Zhang:** Funding acquisition. **Liyong Wu:** Conceptualization, Funding acquisition, Methodology, Writing – review & editing.

Declaration of Competing Interest

The authors declare that they have no known competing financial interests or personal relationships that could have appeared to influence the work reported in this paper.

Acknowledgments

We are grateful to the patients and their families for granting us permission to publish this information. We thank Dr. Pietro Cortelli and Dr. Arturo Garay for their kindly review and constructive suggestions to this study. This work was supported by the Ministry of Science and Technology of China (2019YFC0118600), the National Natural Science Foundation of China (No. 81971011), and the Beijing Municipal Science and Technology Committee (D171100008217005, 7202060).

Appendix A. Supplementary data

Supplementary data to this article can be found online at https://doi.org/10.1016/j.nicl.2022.103026.

References

Ashburner, J., 2007. A fast diffeomorphic image registration algorithm. Neuroimage 38 (1), 95–113.
Chen, S., He, S., Shi, X.-H., Shen, X.-J., Liang, K.-K., Zhao, J.-H., Yan, B.-C., Zhang, J.-W., 2018. The clinical features in Chinese patients with PRNP D178N mutation. Acta. Neurologica Scandinavica 138 (2), 151–155.
Cortelli, P., Perani, D., Montagna, P., Gallassi, R., Tinuper, P., Provini, F.,Gambetti, P., Pre-symptomatic diagnosis in fatal familial insomnia: serial neurophysiological and 18FDG-PET studies, Brain, 129(Pt 3), 668-675, 2006, 10.1093/brain/awl003.
Cortelli, P., Perani, D., Parchi, P., Grassi, F., Montagna, P., De Martin, M., Fazio, F., 1997. Cerebral metabolism in fatal familial insomnia: relation to duration, neuropathology, and distribution of protease-resistant prion protein. Neurology 49 (1), 126–133. https://doi.org/10.1212/wnl.49.1.126.
Gambetti, P., Parchi, P., Petersen, R.B., Chen, S.G., Lugaresi, E., 1995. Fatal familial insomnia and familial creutzfeldt-jakob disease: clinical, pathological and molecular features. Brain 5 (1), 43–51.
Grau-Rivera, O., Calvo, A., Bargalló, N., Monté, G.C., Nos, C., Lladó, A., Molinuevo, J.L., Gelpi, E., Sánchez-Valle, R., Zerr, I., 2016. Quantitative magnetic resonance abnormalities in creutzfeldt-jakob disease and fatal insomnia. J. Alzheimers Dis. 55 (1), 431–443.
Haïk, S., Galanaud, D., Linguraru, M.G., Peoc'h, K., Privat, N., Faucheux, B.A., Ayache, N., Hauw, J.-J., Dormont, D., Brandel, J.-P., 2008. In vivo detection of thalamic gliosis: a pathoradiologic demonstration in familial fatal insomnia. Arch. Neurol. 65 (4), 545.
Hamani, C., Dubiela, F.P., Soares, J.C.K., Shin, D., Bittencourt, S., Covolan, L., Carlen, P. L., Laxton, A.W., Hodaie, M., Stone, S.S.D., Ha, Y., Hutchison, W.D., Lozano, A.M., Mello, L.E., Oliveira, M.G.M., 2010. Anterior thalamus deep brain stimulation at high current impairs memory in rats. Exp. Neurol. 225 (1), 154–162.
He, R., Hu, Y., Yao, L., Tian, Y., Zhou, Y., Yi, F., Zhou, L., Xu, H., Sun, Q., 2019. Clinical features and genetic characteristics of two Chinese pedigrees with fatal family insomnia. Prion 13 (1), 116–123.
Jack, C.R., Wiste, H.J., Weigand, S.D., Therneau, T.M., Knopman, D.S., Lowe, V., Vemuri, P., Mielke, M.M., Roberts, R.O., Machulda, M.M., Senjem, M.L., Gunter, J.L., Rocca, W.A., Petersen, R.C., 2017. Age-specific and sex-specific prevalence of cerebral β-amyloidosis, tauopathy, and neurodegeneration in cognitively unimpaired individuals aged 50–95 years: a cross-sectional study. The Lancet. Neurology 16 (6), 435–444.
Jan, J.E., Reiter, R.J., Wasdell, M.B., Bax, M., 2009. The role of the thalamus in sleep, pineal melatonin production, and circadian rhythm sleep disorders. J. Pineal Res. 46 (1), 1–7. https://doi.org/10.1111/j.1600-079X.2008.00628.x.
Jansen, C., Parchi, P., Jelles, B., Gouw, A.A., Beunders, G., van Spaendonk, R.M.L., van de Kamp, J.M., Lemstra, A.W., Capellari, S., Rozemuller, A.J.M., 2011. The first case of fatal familial insomnia (FFI) in the Netherlands: a patient from Egyptian descent with concurrent four repeat tau deposits. Neuropathol. Appl. Neurobiol. 37 (5), 549–553.
Khan Z.B., Pradeep C., Fatal familial insomnia, NCBI Bookshelf, 2020.
Knopman D.S., Lundt E.S, Therneau T.M, Prashanthi V., Lowe V.J., Kejal K.M., Mary M., Entorhinal cortex tau, amyloid-β, cortical thickness and memory performance in non-demented subjects. Brain(4), 4.
Krasnianski, A., Bartl, M., Sanchez Juan, P.J., Heinemann, U., Meissner, B., Varges, D., Schulze-Sturm, U., Kretzschmar, H.A., Schulz-Schaeffer, W.J., Zerr, I., 2008. Fatal familial insomnia: Clinical features and early identification. Ann Neurol 63 (5), 658–661.
Llorens, F., Zarranz, J.J., Fischer, A., Zerr, I., Ferrer, I., 2017. Fatal familial insomnia: clinical aspects and molecular alterations. Curr. Neurol. Neurosci. Rep. 17 (4), 30. https://doi.org/10.1007/s11910-017-0743-0.
Manetto, V., Medori, R., Cortelli, P., Montagna, P., Tinuper, P., Baruzzi, A., et al., Fatal familial insomnia: clinical and pathologic study of five new cases. Neurology, 42(2), 312-319, 1992, 10.1212/wnl.42.2.312.
Marini, G., Imeri, L., Mancia, M., 1988. Changes in sleep-waking cycle induced by lesions of medialis dorsalis thalamic nuclei in the cat. Neurosci. Lett. 85 (2), 223–227.
Markowitsch H.J., Thalamic mediodorsal nucleus and memory: a critical evaluation of studies in animals and man, Neuroscience & Biobehavioral Reviews, 6, 351-380, 1981.
Mechelli A., Price C.J., Friston KJ., Ashburner J, Voxel-based morphometry applications of the human brain, 2005.
Megelin, T., Thomas, B., Ferrer, X., Ghorayeb, I., 2017. Fatal familial insomnia: a video-polysomnographic case report. Sleep Med. 33, 165–166. https://doi.org/10.1016/j.sleep.2017.02.015.
Montagna, P., 2011. Fatal familial insomnia and the role of the thalamus in sleep regulation. Handb. Clin. Neurol. 99, 981–996. https://doi.org/10.1016/B978-0-444-52007-4.00018-7.
Oh, Y.S., Kim, H.J., Lee, K.J., Kim, Y.I., Lim, S.C., Shon, Y.M., 2012. Cognitive improvement after long-term electrical stimulation of bilateral anterior thalamic nucleus in refractory epilepsy patients. Seizure 21 (3), 183–187. https://doi.org/10.1016/j.seizure.2011.12.003.
Peng, B., Zhang, S., Dong, H., Lu, Z., 2015. Clinical histopathological and genetic studies in a case of FFI with review. Int. J. Clin. Exp. Pathol. 8 (9), 10171–10177.
Provini, F., 2013. Agrypnia excitata. Curr. Neurol. Neurosci. Rep. 13 (4), 341. https://doi.org/10.1007/s11910-013-0341-8.
Rupprecht, S., Grimm, A., Schultze, T., Zinke, J., Karvouniari, P., Axer, H., Schwab, M., 2013. Does the clinical phenotype of fatal familial insomnia depend on PRNP codon 129 methionine-valine polymorphism? J. Clin. Sleep Med. 9 (12), 1343–1345. https://doi.org/10.5664/jcsm.3286.
Shi, X.-H., Han, J., Zhang, J., Shi, Q.i., Chen, J.-M., Xia, S.-L., Xie, Z.-Q., Shen, X.-J., Shan, B., Lei, Y.-J., Shi, S., Zhou, W., Zhang, B.-Y., Gao, C., Liu, Y.-H., Song, J., Guo, Y.-J., Wang, D.-X., Xu, B.-L., Dong, X.-P., 2010. Clinical, histopathological and genetic studies in a family with fatal familial insomnia. Infect. Genet. Evol. 10 (2), 292–297.
Smith, A.T., Cotton, P.L., Bruno, A., Moutsiana, C., 2009. Dissociating vision and visual attention in the human pulvinar. J. Neurophysiol. 101 (2), 917–925. https://doi.org/10.1152/jn.90963.2008.
Sun, C., Xia, W., Liu, Y., Jia, G., Wang, C., Yan, C., Li, Y., 2017. Agrypnia excitata and obstructive apnea in a patient with fatal familial insomnia from China: A case report. Medicine (Baltimore) 96 (49), e8951. https://doi.org/10.1097/MD.0000000000008951.
Tham, W.Y., Thian, Y.L., Ratnagopal, P., Xie, W., 2018. 18F-FDG PET brain in a patient with fatal familial insomnia. Clin. Nucl. Med. 43 (8), e274–e275. https://doi.org/10.1097/RLU.0000000000002152.

Wu, L.-Y., Zhan, S.-Q., Huang, Z.-Y., Zhang, B., Wang, T., Liu, C.-F., Lu, H., Dong, X.-P., Wu, Z.-Y., Zhang, J.-W., Zhang, J.-H., Zhao, Z.-X., Han, F., Huang, Y., Lu, J., Gauthier, S., Jia, J.-P., Wang, Y.-P., 2018. Expert consensus on clinical diagnostic criteria for fatal familial insomnia. Chin. Med. J. 131 (13), 1613–1617.

Watanabe, Y., Funahashi, S., 2012. Thalamic mediodorsal nucleus and working memory. Neurosci. Biobehav. Rev. 36 (1), 134–142.

Van der Werf, Y.D., Witter, M.P., Groenewegen, H.J., 2002. The intralaminar and midline nuclei of the thalamus. Anatomical and functional evidence for participation in processes of arousal and awareness. Brain Res. Rev. 39 (2-3), 107–140.

Van der Werf, Y.D., Witter, M.P., Uylings, H.B.M., Jolles, J., 2000. Neuropsychology of infarctions in the thalamus: a review. Neuropsychologia 38 (5), 613–627.

Zhang, B., Hao, Y.L., Jia, F.J., Shan, Z.X., Wang, S.X., Wing, Y.K., 2010. Fatal familial insomnia: a middle-age-onset Chinese family kindred. Sleep Med 11 (5), 498–499. https://doi.org/10.1016/j.sleep.2009.11.005.